



Proceeding Paper

A Wearable PPG Multi-Sensor for Measurement of Skin Humidity, Temperature, and Contact Pressure [†]

Jiří Přibil *, Anna Přibilová and Tomáš Dermek

Institute of Measurement Science, Slovak Academy of Sciences, Bratislava, Slovak Republic

- * Correspondence: Jiri.Pribil@savba.sk; Tel.: +421-2-59104543
- † Presented at the title, place, and date.

Abstract: The motivation of our work was to analyze influence of changes in humidity and temperature on temporal features of sensed photoplethysmography (PPG) waves. This paper describes a special prototype of a wearable PPG multi-sensor with integrated I2C humidity and thermo meters to carry out measurements in three skin moisture levels. This sensor is supplemented with a force-sensitive resistor for measurement of the physical contact-pressure between the measuring probe and the skin surface next usable to sense heart pulsation on the wrist radial artery. The realized experiments show that the performed skin manipulation (skin drying, moistening) was always detectable; the PPG signal range is mainly affected, while changes in signal ripple and heart rate variance are smaller. The detailed analysis per a hand and gender type yielded differences between male and female subjects, results of left and right hands differ less.

Keywords: contact pressure force measurement; skin humidity and temperature; wearable photoplethysmography optical sensor.

1. Introduction

In the long term, our research is aimed at analysis of influence of examinations based on magnetic resonance imaging (MRI) technique on the mental and physiological state of a tested person [1]. For monitoring of a cardiovascular system including changes in the arterial stiffness and the heart rate (HR) the wearable optical sensors based on the photoplethysmography (PPG) principle have been successfully applied [2], [3]. The current state of the skin surface including humidity, temperature, and other factors can influenced on the precision of PPG wave parameters determined from the sensed PPG signal [4].

Motivation of our work was to analyze the influence of humidity, temperature, and applied contact pressure on temporal features of sensed PPG waves. This paper describes the realization of a special prototype of a wearable PPG multi-sensor with integrated I2C humidity and thermo meters to carry out measurement of a skin condition at the position of an optical sensor. The developed sensor is supplemented with a force-sensitive resistor (FSR) element enabling to measure the contact pressure between the PPG sensor probe and the skin surface. The FSR component is also applicable to measure the heart pulsation on the wrist radial artery and to perform comparison of HR values determined from a PPG signal [5], [6]. Due to its planned use in experiments inside the scanning area of an MRI tomograph [7], also the current sensor prototype consists of non-ferromagnetic materials and all parts are shielded by aluminum boxes.

After verifying the sensor's functionality in laboratory conditions, the stability and quality of wireless Bluetooth (BT) connection was tested in an environment of the scanning MRI device and the measurement of the received signal strength indicator (RSSI) parameter was performed. The main measuring experiment consists of PPG signal sensing on a wrist for different levels of skin moisture (by washing a hand, by drying a skin, etc.) before each of the measuring phases. The database of sensed data records collected in this way was next statistically analyzed with the final aim – to make some practical recommendation from the point of view of humidity and temperature changes during long-time experiments inside the MRI device.

2. Methods

2.1. PPG Signal Description and Features Determination

Generally, the optical PPG sensor can work on a transmittance or reflectance principle. The transmittance type of the sensor probe has usually a form of a finger ring with a light source (one or more LED elements) and a photo detector placed on opposite sides of the sensed human tissue – this realization is mainly applied in pulse oximeter devices. In the case of the reflectance type, a photo detector measures the intensity of the light reflected from the skin and it is placed on the same side of the skin surface as a light source transmitter. The reflectance PPG sensors are worn typically on fingers or wrists as a part of wearable devices – fitness bracelets, smart watches, etc. [8]. In both types the picked-up PPG signal contains two local maxima representing systolic and diastolic peaks providing valuable information about the pumping action of the heart. Three types of sensed PPG signals can be classified: a raw pulse wave, and its first/second derivative (FD/SD-PPG). While the raw PPG signal does not seem suitable for local maxima determination, the firstorder and the second-order derivatives are more informative due to more pronounced local extrema [9]. Therefore, for the purpose of the PPG pulse wave analysis, the PPG signal derivatives are usually calculated. The amplitude of the sensed PPG signal is usually not constant but modulated and it can be often partially disturbed or degraded. For this reason, some de-trending and filtering operations must be applied on the picked-up PPG signal before its analysis [10].

For description of PPG signal properties, the energetic, time, and statistical parameters should be determined. First, the upper and lower envelopes ($E_{\rm HI}$, $E_{\rm LOW}$) are calculated by low pass filtering of the squared input signal. In the case of the SD-PPG wave the $E_{\rm HI}$ corresponds with the systolic peaks, and the $E_{\rm LOW}$ with the diastolic ones. While the absolute difference between $E_{\rm HI}$ and $E_{\rm LOW}$ mean values ($\mu E_{\rm HI} - \mu E_{\rm LOW}$) represents the PPG signal range ($HP_{\rm RANGE}$), the heart pulses ripple in percentage is calculated as $HP_{\rm RIPP}$ = ((max $E_{\rm HI}$ - min $E_{\rm HI}$) / $\mu HP_{\rm RANGE}$) × 100 using maximum and minimum values of the upper envelope $E_{\rm HI}$ and the mean signal range. Next, the localized peak positions $P_{\rm SYS}$ are applied to determine the heart cycle periods $T_{\rm HP}$ (in samples) and using the sampling frequency $f_{\rm S}$ in Hz, the heart rate in min⁻¹ is evaluated as HR = 60 / ($T_{\rm HP}$ × $f_{\rm S}$). For further comparison, the relative variance $HR_{\rm RVAR}$ in percentage based on the mean (μ HR) and the standard deviation (σ HR) values can be also calculated as $HR_{\rm RVAR}$ = σ HR/ μ HR × 100.

2.2. Sensing and Analysis of Humidity and Temperature Values

Humidity sensors operate on the principle of change in the electrical impedance (capacitance) with varying moisture levels. The sensor's active component, typically a hygroscopic substance (a material that absorbs water or water vapor) [11]. Changes of a dielectric constant generated in this way are detected and expressed as a change in relative humidity (RH in %). Some prototypes of humidity and temperature sensors were developed for special experimental purposes in the biomedical research [12], [13]. An easy way

is to use a commercial monolithic chip with integrated humidity and temperature sensors which include also an analog-to-digital converter (ADC) and an I2C interface. This chip next performs signal processing, data calibration including polynomial non-linearity correction, and hysteresis effect minimization [14]. Therefore, each time of the RH measurement is made, the temperature is measured too, for the purpose of temperature compensation. It means, the temperature T1 values are at disposal in parallel with the RH ones.

To map relative humidity and temperature changes during the measurement with the time duration t_{DUR} , the linear trend is calculated from the obtained RH and T1 sequences (RH_{LT} and $T1_{\text{LT}}$) by the linear least squares fitting technique. Next, the differences Δ RH and Δ T1 between values taken at the start and the end of the measurement phase can be determined. Finally, the gradient parameter defined as the ratio $RH_{\text{GRAD}} = (\Delta RH / t_{\text{DUR}})$ [%/ s] and $T1_{\text{GRAD}} = (\Delta T1 / t_{\text{DUR}})$ [°C / s] can be successfully used for evaluation and comparison. The positive linear trends RH_{LT} and $T1_{\text{LT}}$ as well as gradient values represent the increasing trend; the negative ones signify the decreasing trend.

2.3. Contact Pressure Determination using an FSR Element

From a physical point of view, the FSR element is realized in the form of a flexible thin film pressure resistive sensor. The output resistance decreases as the pressure on the sensor surface increases [15]. There is typically a non-linear relationship between the output resistance $R_{\rm FSR}$ in k Ω and the applied pressure in kg. Therefore, in praxis, the conductance $G_{\rm FSR}$ =1/ $R_{\rm FSR}$ is often used for building of the pressure characteristic. For pressure measurement based on an FSR component, the voltage divider is usually applied. Its supplementary resistor R1 is wired either as a push-up component connected to the power supply or as the pull-down resistor connected to the ground. The output analogue signal $V_{\rm OUT}$ from both types of voltage dividers depends on the actual value after A/D conversion ($V_{\rm ADC}$), resolution $AD_{\rm RES}$ of the used ADC, and applied powering voltage $V_{\rm CC}$ as $V_{\rm OUT}$ = $V_{\rm ADC} \times V_{\rm CC}/AD_{\rm RES}$. When the R1 is in the role of a push-down resistor, the resistance of the FSR element is R_0 = $R_1 \times (V_{\rm CC}/V_{\rm OUT} - 1)$, otherwise R_0 = $R_1 \times (1 - V_{\rm CC}/V_{\rm OUT})$.

The FSR element can be also used for sensing of the blood pulsation in a vessel (on a wrist), and it can be compared with PPG signals based on an optical principle. When the sufficient contact pressure of the PPG sensor is applied on a vessel skin, a pulsation in the rhythm of systolic peaks of the PPG wave is well detectable (see an example in Figure 1b). On the other hand, too low pressure generates the PPG signal with lower range and the diastolic pulse part is not well expressed (see the graph in Figure 1a), while too strong pressure applied can degrade and compress the PPG signal taken from a vessel as documented by the graph in Figure 1c. In this way, HR values ($HR_{\rm FSR}$) and FSR signal parameters (range – $FSR_{\rm RANGE}$, mean – μ FSR, and std – σ FSR values) can be next determined. For mapping of the correlation between heart rates determined from the PPG signal ($HR_{\rm FPG}$) and $HR_{\rm FSR}$ values, the Pearson correlation coefficient Rcc can be calculated, and the scatter plot can be used for visualization.

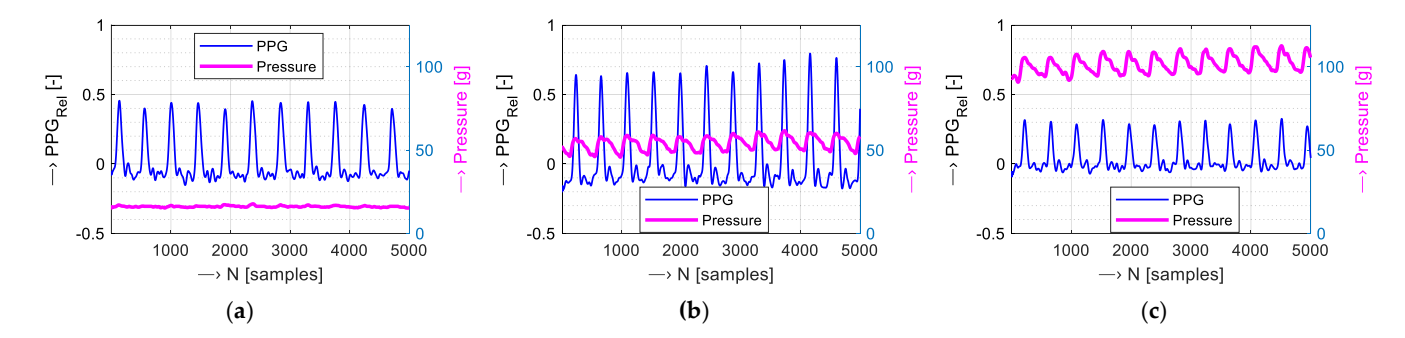


Figure 1. Example of a 5-k sample PPG wave with a pressure signal measured in parallel by an FSR element: (a) with too low-pressure level, (b) with proper pressure value, (c) with too high pressure applied; all signals taken on the left wrist, f_s =500 Hz.

3. Objects, Experiments, and Results

3.1. Structure and Realization of a Wearable PPG Multi-Sensor

The currently realized prototype of a wearable PPG multi-sensor (further call as "PPGs-HTF") consists of two basic parts: the measuring probe and the sensor's body with a battery cell for powering. The measuring probe contains the following components:

- the reflectance optical PPG sensor with fully integrated analogue interface the Pulse Sensor Amped (Adafruit 1093) [16] by Adafruit Industries, NY, USA;
- the Adafruit Si7021 Temperature & Humidity I2C Sensor (Adafruit 3251 STEMA QT) [14] by Adafruit Industries, NY, USA;
- the Force Sensitive Resistor sensor Whadda WPSE477 [17] product by Velleman Group NV, Gavere, Belgium.
- As an FSR single point sensor was used the WPSE477 type with a 7.62 mm diameter sensing area, 0.2 mm thickness, measure range up to 0.5 kg (lower pressure threshold < 20 g), and a declared accuracy of ±2.5 % (in the 85% range interval) [17]. The Si7021 chip can measure the relative humidity in the range of 0-80% RH with an accuracy of ±3% and the temperature from -10°C to +85°C with a typical accuracy of ±0.4°C [14].
- The sensor's body is based on the Arduino compatible micro-controller board Adafruit Feather 328P by Adafruit Industries, NY, USA, using the processor AT-mega328P by Atmel Company, running at 3.3V logic and 8 MHz, with eight 10-bit ADCs, including also hardware I2C, and SPI support, hardware USART to USB (CP2104) converter, and 100 mA charger for Lithium polymer (Li-Po) batteries [18]. Here is also located the bi-directional communication BT module MLT-BT05 by Techonics Ltd, Shenzhen, China, working in the BT4.0 BLE standard at 2.4 GHz. The whole sensor is normally powered by a 3.7 V Li-Po battery, but it is also possible to use the 5V USB port for the purpose of micro-controller programming or debugging, and first of all for charging of a battery cell. To enable measurements in a scanning area of a running MRI device, both parts of this wearable PPG multi-sensor consist of non-ferromagnetic components, and it is shielded by aluminum boxes see assembling photos in Figure 2.

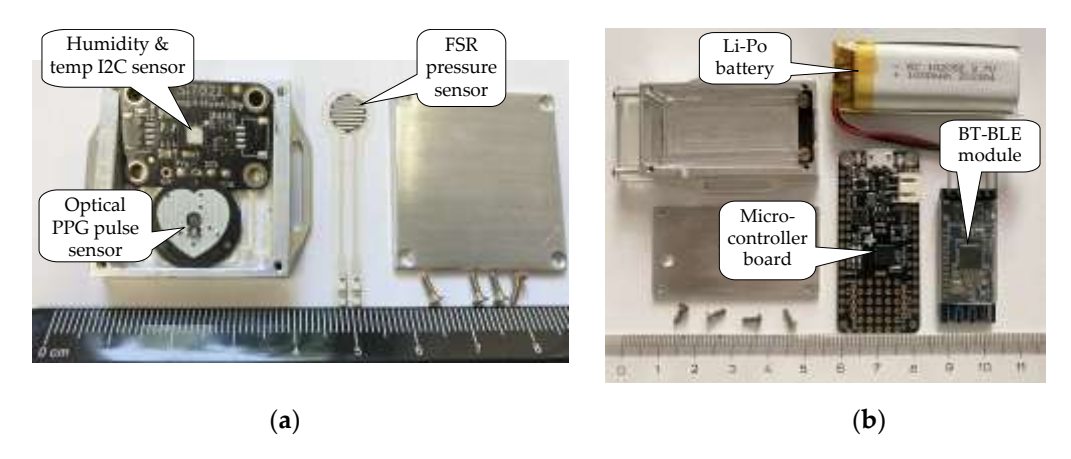


Figure 2. Construction of the PPGs-HTF sensor assembling: (a) photo of a measuring sensor part, (b) photo of a sensor's body including a Li-Po battery.

3.2. Auxiliary Experiments and Investigations

After verifying the sensor's basic functionality in the normal laboratory conditions, was performed testing the stability of wireless communication and quality of BT connection between the sensor and the control laptop in three conditions:

- MRI device is ready to scan, but no MR sequence is running open shielding cage door (Cond1);
- closed cage door without MR scanning (Cond2);
- the MR scan sequence is executed the door must be closed (Cond3).

The quality of wireless communication was evaluated in a low magnetic field environment of the open-air MRI device E-scan Opera by Esaote S.p.A., Genoa, Italy, based on a low static magnetic field of 0.178 T located at our Institute [19]. The tested multi-sensor was present inside the scanning area of the MRI device; the control laptop was situated outside the shielding metal cage - see the overall photo in Figure 3. During this measurement a testing spherical water phantom was placed in the RF receiving/transmitting coil, no person was really investigated. To obtain also a signal from the FSR component, the measuring probe was fixed on a plastic cube (simulating of a human wrist) by a polyamide ribbon - see the detail in Figure 3. The distance between the sensor and the control device was approx. 2.5 m, the bi-directional BT communication was operated at a rate of 57600 bps. In the frame of the third testing condition, the MR scan 3D-CE sequence was running [19]. The quality of the BT connection can be evaluated by the received RSSI parameter representing an estimated measure of the power level received by a radiofrequency (RF) client device from an access point [20]. In our case, the RSSI values in dBm were obtained in the frame of the BT BLE connection establishment. The mean and std RSSI values calculated from five measurements per each testing condition are shown in Table 1.

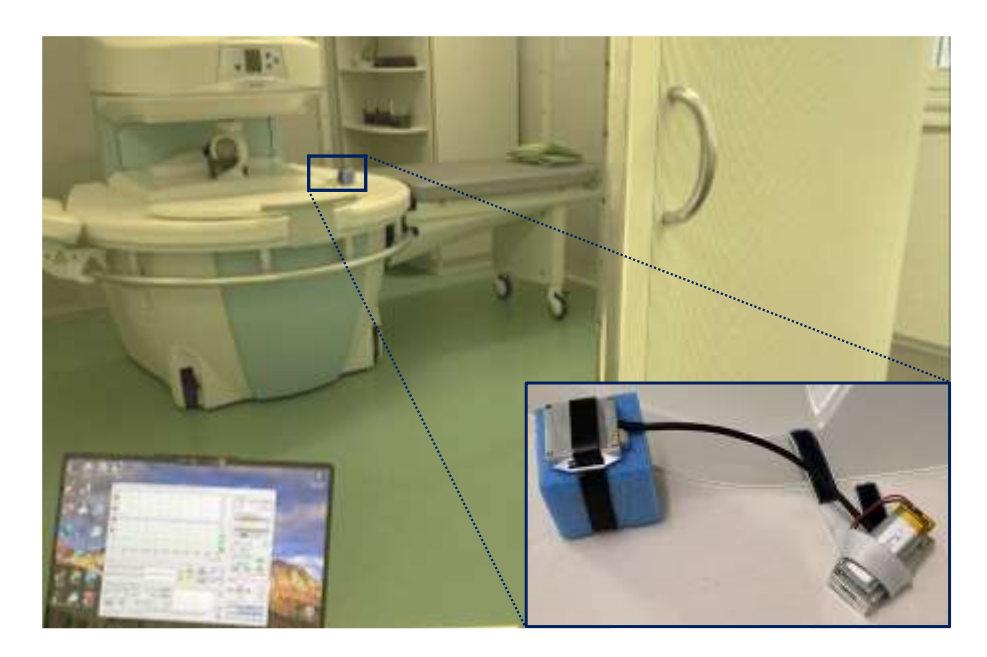


Figure 3. Arrangement of RSSI measurement inside the MRI device E-Scan Opera located in the metal shielding cage and a control laptop in front of the open cage door.

Table 1. Mean and std RSSI values measured in three conditions inside the E-Scan Opera device.

| BT module / condition | Cond1 | Cond2 | Cond3 |
|-----------------------|-----------------------------|-----------------------------|-----------------------------|
| MLT-BT05 A) | $-86.2 \pm 0.3 \text{ dBm}$ | $-92.3 \pm 0.5 \text{ dBm}$ | $-93.7 \pm 0.8 \text{ dBm}$ |

^{A)} the BT BLE module working in BT 4.1 standard, serial communication operated at 57600 bps.

3.3. The Main Measurement Experiment

The main measurement experiment consists of real-time sensing of PPG waves, humidity and temperature values together with the information about the current contact pressure applied on the skin surface by a measuring probe. The tested person was sitting with a hand laid on a table in a normal office room. The measuring probe was worn on the wrist artery of the left or right hand, while the sensor's body was fixed on the upper part of the arm (see the arrangement photo in Figure 4). The measurements were realized for three skin moisture levels:

- the sensor's probe was worn without any adjustment of the skin surface of the bottom wrist area (Normal);
- the skin surface is dried by a handkerchief (Dry);
- the skin is partially moistened by a wet cloth before the probe wearing (Wet).

The real-time measurements were performed in the following phases:

- 1. Preparation phase (M0) without any practical measurement, when the body of the PPG multi-sensor is mounted on the tested person's arm, BT connection with the control device is established, and the quality of the sensed PPG and pressure (FSR) signals is verified. Next, some adjustment of the skin surface is performed depending on the required skin moisture level.
- 2. The initial 90-sec measurement phase M1, when the RH and T1 values are taken in the intervals of T_{INT} = 1 s. In the first 30 seconds of this duration, the measuring probe is freely laid on the desk (current air conditions are measured) and then the probe is put on the left/right wrist of the tested person. At this moment, the offset of RH and T1 sequences (RH_{OFS} and $T1_{\text{OFS}}$) are determined.
- 3. In phase M2 with the time duration of 256 sec, the PPG and FSR analog signals (sensed using the sampling frequency $f_S = 125 \text{ Hz}$) together with RH and T1 values (with $T_{\text{INT}} = 0.2 \text{ s}$ intervals) are recorded in parallel.

4. The final 90-sec measurement phase M3 starts in the moment when the measuring probe is put off from a wrist. In this case the RH and T1 values are again recorded using $T_{\text{INT}} = 1 \text{ s}$.

The total time duration of the whole measurement is approx. 8÷10 minutes – depending on the length of the preparation part. The total number of the detected heart periods $N_{\rm HP}$ usable for calculation of HR values ($HR_{\rm PPG}$ and $HR_{\rm FSR}$) depends on the actual state of a tested person during the measurement phase M2. The span changes of RH and T1 sequences during the measuring experiment with the sensor's probe put on the skin is calculated as the difference Y (RH or T1): $\Delta Y_{\rm PON} = Y_{\rm MZE} - Y_{\rm OFS}$. Here $Y_{\rm MZE}$ represents the last value received from the Si7021 chip in the phase M2 ($RH_{\rm MZE}$ and $T1_{\rm MZE}$) and $Y_{\rm OFS}$ is the offset value taken in about the 30th second of the M1 phase.

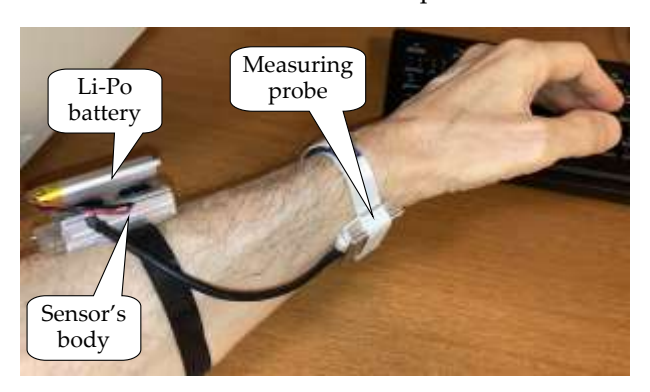


Figure 4. Principal arrangement photo of the main measurement experiment.

During our experiments a small database of real-time signal records was collected. It originated from seven non-smoker right-hand dominated volunteers (four males $P1_M-P4_M$ and three females $P1_F-P3_F$) with a mean age of 52 ± 18 years. The collected data records consist of 6 files per a person in total – two from M1 and M3 phases and one from the phase M2, picked-up on the left and right hands. They were subsequently processed offline to determine PPG and FSR signal properties and changes in RH and T1 sequences within all measuring phases M1-3.

The following example describes determination of PPG signal properties together with parameters of RH and T1 sequences taken from the right hand of a male testing subject P1M with the wet skin moisture level. Concatenated RH and T1 sequences for the measuring phases M1-3 with denoted time stamps of the measuring probe putting on and off, determined offset levels RHoFS and T1oFS and final span changes $\Delta RHFON$ and $\Delta T1FON$ can be seen in Figure 5. Comparison of sequences of HR values determined from PPG and FSR signals is shown in Figure 6a, the scatter-plot in Figure 6b together with the calculated Rcc coefficient describing correlation between HRFFSC and HRFSC sequences. Table 2 enumerates partial results for all three tested skin moisture levels. Box-plots in Figure 7 compare differences in statistical properties of $\Delta RHFON$, and $\Delta T1FON$ parameters for three skin moisture levels, categorized by the type of the used hand and the gender of the tested person separately. Figure 8 presents summary mean results for all tested subjects visualized as bar-graphs for tracking changes in five most important PPG signal properties – HPRANCE, HPRIPP, HR relative variance (HR1 from HRFPPC, HR2 from HRFSC values), and Rcc.

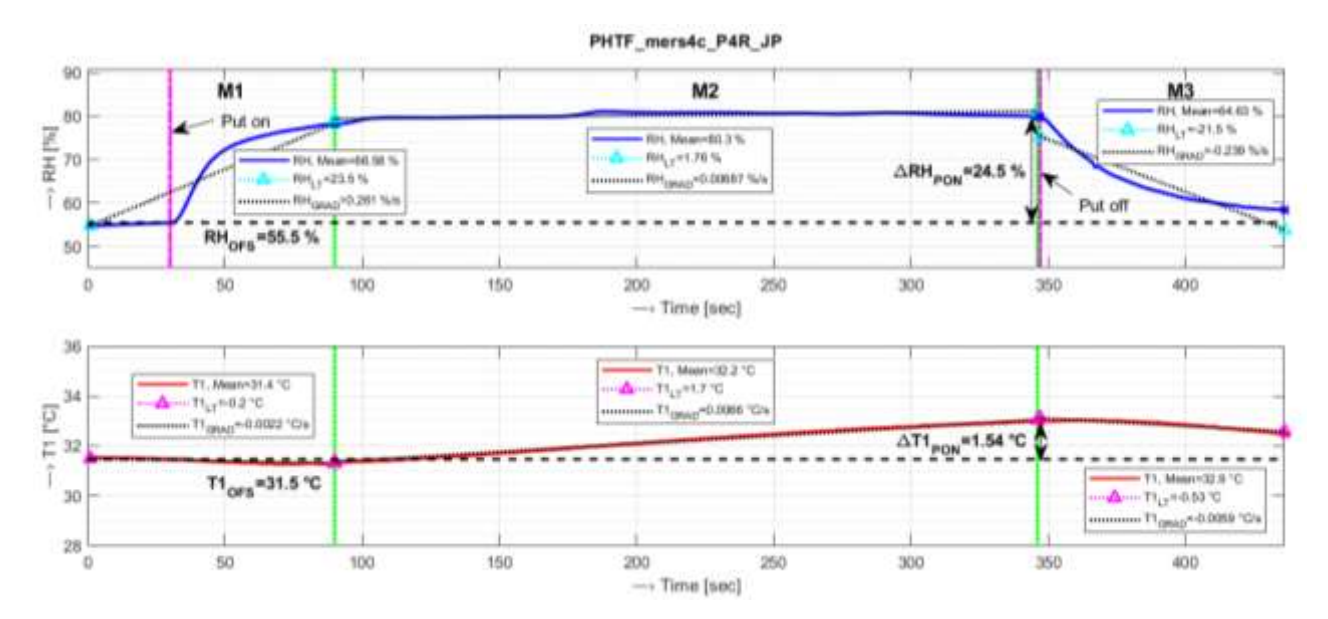


Figure 5. Concatenated RH (upper graph) and T1 (lower graph) sequences for measuring phases M1-3 taken in the wet skin moisture level with denoted time stamps of the measuring probe putting on and off, determined offset levels, and final span changes; right hand of the subject P1_M.

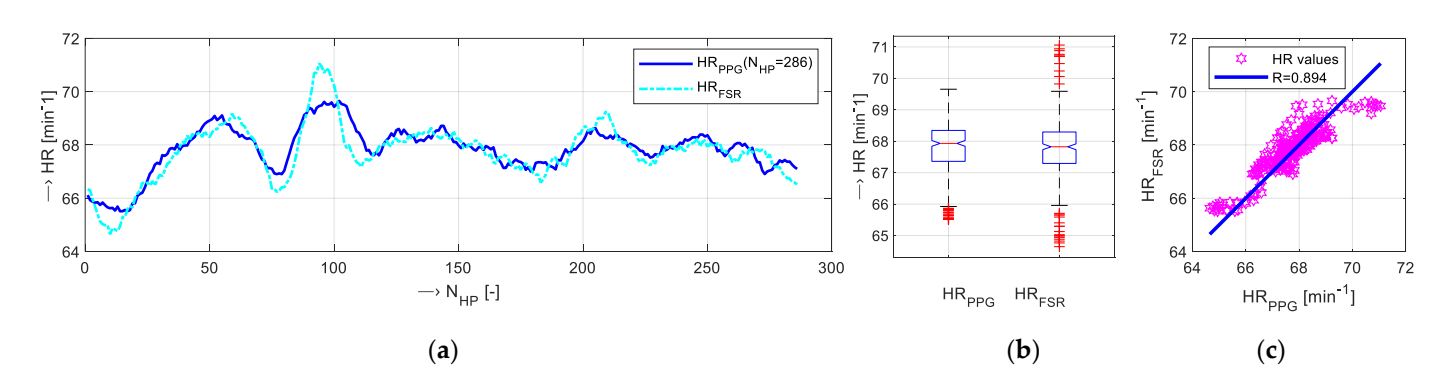


Figure 6. Comparison of *HR*_{PPG} and *HR*_{FSR} values: (a) visualization of *HR*_{PPG} and *HR*_{FSR} sequences, (b) box-plot of basic statistical parameters, (c) the scatter-plot together with the calculated Pearson correlation coefficient *Rcc*.

Table 2. Partial results of PPG signal properties and HR statistical features for three skin moisture levels; right hand of the subject P1_M.

| Condition | <i>HP</i> RANGE A) [-] | HPRIPPLE [%] | HR1 _{RVAR B)} [%] | HR2 _{RVAR} ⁽²⁾ [%] | Rcc [-] |
|-----------|------------------------|--------------|----------------------------|--|---------|
| Normal | 35.2 | 29.1 | 2.09 | 2.21 | 0.968 |
| Wet | 20.4 | 26.6 | 1.65 | 1.79 | 0.941 |
| Dry | 25.7 | 26.6 | 1.29 | 1.58 | 0.894 |

^{A)} Measuring probe put on with the applied mean $CP \cong 100$ grams.

Calculated from HR_{PPG} . Calculated from HR_{FSR} .

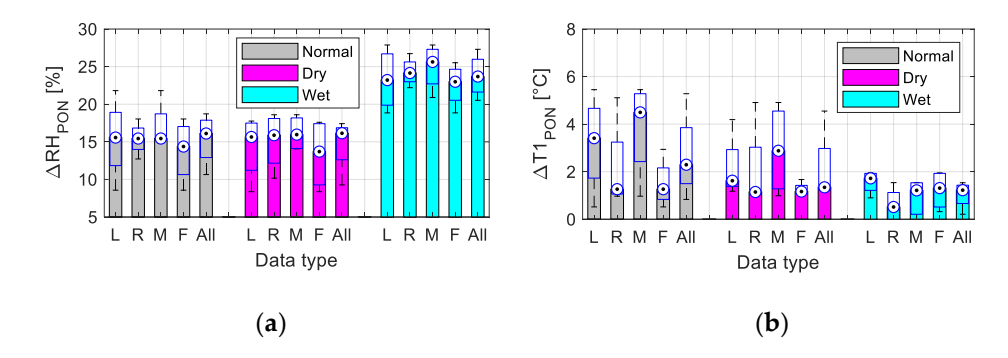


Figure 7. Basic statistical properties compared per the type of the used hand (Left/Right) and the gender of the tested subject (Male/Female) and summary ones (All) for three skin moisture levels: (a) ΔRH_{PON} , (b) $\Delta T1_{PON}$ parameters

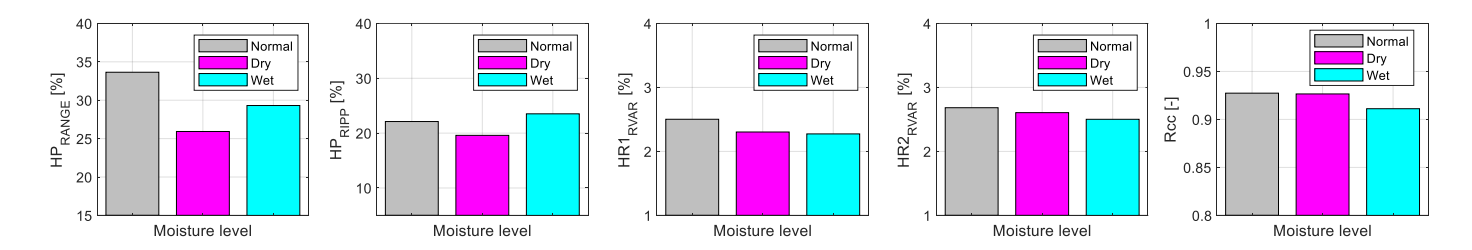


Figure 8. Bar-graphs of summary mean results for both hands and all tested subjects (from **left** to **right):** values of HP_{RANGE} , HP_{RIPP} , HR relative variance (HR1 from HR_{PPG} , HR2 from HR_{FSR}).

4. Discussion and Conclusions

The performed measurement confirms functionality of the developed special prototype of a wearable multi-sensor enabling measurement of PPG signals, relative humidity, temperature values, and contact pressure by an FSR element. Auxiliary experiments check the practical possibility of wireless BT connection and data transfer through the shielding cage of the open-air MRI device, but with lower signal intensity (compare values in Table 1). The minimum RSSI of –94 dBm was reached when the cage door was closed and an MR scan sequence was running, but the BT connection was always stable, the real-time data transfer was still functional, and the received data of analogues signals were usable for further processing and analysis.

Principally, there exist differences between skin properties of male and female subjects. Female skin has generally slightly thinner capillaries, so lower contact pressure must be applied to obtain a proper signal from the FSR sensor – suitable for HR values detection and comparison with values obtained from the PPG signal. Therefore we finally tried to apply the mean contact pressure of μ CP=100 gram for the male tested persons and μ CP=75 gram for the female ones.

The obtained results of realized main measuring experiments show that the performed skin manipulation (skin drying and/or moistening) was well detectable in all cases – see changes of ΔRH_{PON} parameter in Figure 7. As it can be seen here, when the moistening was applied, the highest ΔRH_{PON} values were achieved. From the point of view of $\Delta T1_{PON}$ parameters the situation is opposite – skin moistening produces the smallest values. The detailed statistical analysis performed separately per hand and gender types (see box-plots in Figure 7) documents that there exist differences in ΔRH_{PON} values between results of male and female tested subjects, but results of measurements on the left and right hands differ less(not much significantly). In the case of $\Delta T1_{PON}$ parameter, obtained

values differs significantly for gender as well as the hand type. These conclusions must be confirmed by further experiments – at present a small number of measurements on subjects was realized (four males and three females only).

As it is confirmed by visualization of concatenated RH and T1 sequences for measuring phases M1 and M3, the 90-sec time duration of F1 and F3 measuring phases was chosen properly – during the main measuring phase M2 the changes of RH are minimal (see upper graph in Figure 7). In the case of temperature skin changes which are affected for a longer time, small increase of T1 values can be observed within the M2 phase. The proposed return of T1 values to the offset level during the M3 phase was not practically fulfilled as shown in the lower graph in Figure 5. For this reason, about one minute time delay was finally applied before next measurement with different skin moisture level to minimize this undesirable effect.

Different skin moisture levels are mainly expressed by changes in HP_{RANGE} parameter (see the left bar-graph in Figure 8). Skin drying affects decrease of heart pulse range, while moistening brings increase of PPG signal ripple. Skin manipulation has not directly influence on the variance of the calculated HR values (obtained mean HR variance values are comparable/similar), but in all cases the HRs determined from the FSR signal have higher HR2RVAR. The smallest Rcc values (HRPPG and HRFSR differing mostly) were obtained after skin moistening operation, as documented by the right bar-graph in Figure 8. So far we cannot find any explanation for this effect; the planned more measuring experiments in the near future could also cover this phenomenon.

Author Contributions: Conceptualization and methodology, J.P., A.P.; data collection and processing J.P. and T.D., HW realization and testing, J.P. and T.D.; writing—original draft preparation, J.P. and A.P.; writing—review and editing, A.P.; project administration, J.P.; funding acquisition, J.P. All authors have read and agreed to the published version of the manuscript.

Funding: This work was funded by the Slovak Scientific Grant Agency project VEGA2/0004/23.

Institutional Review Board Statement: Institutional review board statement was waived for this study, due to testing authors themselves and colleagues from IMS SAS. No personal data were saved, only PPG signals, contact pressure force values, and skin humidity and temperatures sensed on left/right wrists were used in this research.

Informed Consent Statement: Not applicable. **Data Availability Statement:** Not applicable.

Conflicts of Interest: The authors declare no conflict of interest.

References

- 1. Mechefske, C.K. Acoustic noise in MRI scanners. In *Biomedical Applications of Vibration and Acoustics in Therapy, Bioeffect and Modeling*; ASME: New York, NY, USA, 2008; pp. 275–328.
- 2. Dieffenderfer, J.; Goodell, H.; Mills, S.; McKnight, M.; Yao, S.; Lin, F.; Beppler, E.; Bent, B.; Lee, B.; Misra, V.; Zhu, Y. Low-Power Wearable Systems for Continuous Monitoring of Environment and Health for Chronic Respiratory Disease. *IEEE J. Biomed. Health Inform.* **2016**, *20*, 1251–1264. https://doi.org/10.1109/JBHI.2016.2573286.
- 3. Charlton, P.H., Marozas, V. Wearable photoplethysmography devices. In *Photoplethysmography: Technology, Signal Analysis, and Applications*; Kyriacou, P.A., Allen, J.; Eds.; Elsevier: London, UK, 2022; pp. 401–438.
- Kazanskiy, N.L.; Butt, M.A.; Khonina, S.N. Recent Advances in Wearable Optical Sensor Automation Powered by Battery versus Skin-like Battery-Free Devices for Personal Healthcare—A Review. Nanomaterials 2022, 12, 334. https://doi.org/10.3390/nano12030334
- 5. D'Acquisto, L.; Scardulla, F.; Montinaro, N.; Pasta, S.; Zangla D.; Bellavia, D. A preliminary investigation of the effect of contact pressure on the accuracy of heart rate monitoring by wearable PPG wrist band. In *II Workshop on Metrology for Industry 4.0 and IoT*; MetroInd4.0&IoT: Naples, Italy, 2019; pp. 334-338. https://doi.org/10.1109/METROI4.2019.8792834.

- Scardulla, F.; D'Acquisto, L.; Colombarini, R.; Hu, S.; Pasta, S.; Bellavia, D. A Study on the Effect of Contact Pressure during Physical Activity on Photoplethysmographic Heart Rate Measurements. Sensors 2020, 20, 5052. https://doi.org/10.3390/s20185052.
- 7. Přibil, J., Přibilová, A., Frollo, I. First-step PPG signal analysis for evaluation of stress induced during scanning in the open-air MRI device. *Sensors* **2020**, *20*, 3532. https://doi.org/10.3390/s20123532.
- 8. Scardulla, F. et al. Photoplethysmograhic sensors, potential and limitations: Is it time for regulation? A comprehensive review. *Measurement* **2023**, 218, 113150. https://doi.org/10.1016/j.measurement.2023.113150.
- 9. Nitzan, M., Ovadia-Blechman, Z. Physical and physiological interpretations of the PPG signal. In *Photoplethysmography: Technology, Signal Analysis, and Applications*; Kyriacou, P.A., Allen, J., Eds.; Elsevier: London, UK, 2022; pp. 319–339, ISBN: 978-0-12-823374-0.
- 10. Elgendi, M. PPG Signal Analysis: An Introduction Using MATLAB; CRC Press: Boca Raton, FL, USA, 2021; pp. 27–36, ISBN 978-1-138-04971-0.
- 11. Humidity Sensor–Types and Working Principle. June 7, 2024 By Bala, © 2024 Electronicshub.org. Available online: https://www.electronicshub.org/humidity-sensor-types-working-principle/ (accessed on 1 June 2025).
- 12. Huang T.-H., Chou, J.-C., Sun, T.-P., Hsiung, S.-K. A device for skin moisture and environment humidity detection. *Sens. Actuators B Chem.* **2008**, 134, 206–212. https://doi.org/10.1016/j.snb.2008.04.030.
- Volkova, E.; Perchik, A.; Pavlov, K.; Nikolaev, E.; Ayuev, A.; Park, J.; Chang, N.; Lee, W.; Kim, J.Y.; Doronin, A.; Vilenskii, M. Multispectral sensor fusion in SmartWatch for in situ continuous monitoring of human skin hydration and body sweat loss. Sci. Rep. 2023, 13, 13371. https://doi.org/10.1038/s41598-023-40339-7.
- 14. Si7021-A20 Data Sheet-I2C Humidity and Temperature Sensor, Rev. 1.3 6/22. © 2022 by Silicon Laboratories. Available online: https://www.silabs.com/documents/public/data-sheets/Si7021-A20.pdf (accessed on 15 June 2025).
- 15. FSR Integration Guide & Evaluation Parts Catalog with Suggested Electrical Interfaces, Version 1.0, 90-45632 Rev. D, 24 p., Interlink Electronics Inc., Camarillo, Canada. Available online: https://www.sparkfun.com/datasheets/Sensors/Pressure/fsrguide.pdf (accessed on 26 April 2024)
- 16. Pulse Sensor Amped Product (Adafruit 1093): World Famous Electronics Ilc. Ecommerce Getting Starter Guide. Available online: https://pulsesensor.com/pages/code-and-guide (accessed on 16 July 2020)
- FSR Sensor Module Whadda WPSE477–Manual Velleman. Available online: https://cdn.velleman.eu/downloads/25/prototyp-ing/manual_wpse477.pdf (accessed on 15 June 2025).
- 18. Adafruit Feather 328P by Ada, Last Edited August 23, 2024. Available online: https://cdn-learn.adafruit.com/down-loads/pdf/adafruit-feather-328p-atmega328-atmega328p.pdf (accessed on 15 June 2025)
- 19. E-Scan Opera. Image Quality and Sequences Manual; Revision 830023522; Esaote S.p.A.: Genoa, Italy, 2008.
- 20. RSSI-Received Signal Strength Indication. Available online: https://www.rfwireless-world.com/Terminology/RSSI-Received-Signal-Strength-Indication.html (accessed on 3 February 2024).

Disclaimer/Publisher's Note: The statements, opinions and data contained in all publications are solely those of the individual author(s) and contributor(s) and not of MDPI and/or the editor(s). MDPI and/or the editor(s) disclaim responsibility for any injury to people or property resulting from any ideas, methods, instructions or products referred to in the content.